https://doi.org/10.1016/j.scs.2023.104735

Techno-economic evaluation and environmental benefit of hybrid evaporative cooling system in hot-humid regions

Abstract

Reducing the energy consumption of buildings is of great importance to achieve carbon neutrality targets. The air conditioning (AC) system in buildings, as a large energy consumer, should be taken into account as one of the main building service systems for energy saving integrated with energy-efficient and environmental-friendly technologies. Indirect evaporative cooler (IEC), constrained by its cooling principle, originally exerts energy saving potential in hot-arid regions. Recently, progress has been made in expanding its application to hot-humid regions. However, due to the large cooling load in hot-humid regions, an IEC-integrated hybrid system should be developed as an improved solution to effectively save energy and maintain the indoor thermal comfort. In view of the lack of a complete hybrid IEC system being reported thus far, in this study, the IEC is combined with a cooling coil unit as a primary air handling unit (IEC-PAU) for fresh air handling and supply. Accordingly, the model of the IEC-PAU with indoor fan coil units (FCUs) is constructed and incorporated into a typical office building, and the results are compared with a baseline case under hot-humid climate conditions. Comprehensive energy, economic, and environmental benefits are analyzed considering different setpoint temperatures in typical cities of the Great Bay area (GBA) of China. Results show that the proposed system could reduce the energy consumption of 4.6 kWh/m^2 on average, with the acceptable thermal comfort level as they are in the reference cases. The greatest energy saving ratio is 8.3%, while the performance of the proposed system declines under the higher setpoint temperature. The saved

electricity expenses can lead to the average discounted payback period of 8.2 years in the GBA cities. Furthermore, an annual greenhouse gas emission of 4.8 t on average can be diminished. In summary, this work demonstrates the feasibility of the hybrid IEC system as an effective approach for energy saving in hot-humid regions, which is promising to prompt the carbon neutrality in China.

Keywords

Air conditioning; Hybrid indirect evaporative cooling system; Hot and humid regions; Energy saving; Economic and environmental benefit

Nomenclature

C_I	Initial investment, CNY
C_{net}	Net cash flow, CNY
$f_{emission}$	Greenhouse gas emission intensity, kg CO_2 e/kWh
m_{ratio}	Mass ratio of secondary air to primary air
E	Energy saving, kWh
$M_{emission}$	CO_2 emission, t
r	Discount rate
j	Service life of the device, year
L	Length, m
W	Width, m
H	Height, m
m	Mass flow rate, m^3/s

Abbreviations

AC	Air conditioning
DEC	Direct evaporative cooling
DPP	discounted payback period
FCU	Fan coil unit
GBA	Great Bay Area
HKD	Hong Kong dollar
IEC	Indirect evaporative cooling
LD	Liquid desiccant
MOP	Macau pataca
NPV	Net present value
PAU	Primary air handling unit

Greek symbols

η_{wb}	Wet-bulb efficiency
ε_{de}	Dehumidification rate

PMV	Predicted mean vote
PPD	Predicted percentage of dissatisfied
SHGC	Solar heat gain coefficient

1. Introduction

Achieving the carbon peak and carbon neutrality requires the transformation of the energy system and the reduction of energy use for an economy (Liu, Liu, Jiang, Zhang, & Hao, 2022). In the building sector, different building service systems offer various functions for human activities and consume energy. The air conditioning (AC) system regulates indoor thermal comfort and provides fresh air for occupants. However, the widespread application of mechanical vapor compression (MVC) devices has led to significantly increased energy consumption (Men, Liu, & Zhang, 2021). To address this issue, in addition to relying on advanced control strategies and variable drive technologies, some scholars pay attention to the daily physical process to handle hot fresh air. Evaporative cooling is one of the ways to remove heat through water evaporation for fresh air supply, which is a sustainable cooling approach without harmful chemical refrigerants and is popular to reduce energy consumption and greenhouse gas emission in hot-arid regions (Abaranji, Panchabikesan, & Ramalingam, 2021; Mirzazade Akbarpoor, Moghtader Gilvaei, Haghighi Poshtiri, & Zhong, 2022; Sun et al., 2023; Tariq et al., 2021). Nevertheless, the traditional direct evaporative cooling (DEC) lowers ambient air temperature at the expense of increased humidity, rendering it unsuitable for high-humidity regions. Consequently, indirect evaporative cooling (IEC) is adopted as an alternative (Shi, Min, Ma, Chen, & Yang, 2022a; Yang, Shi, Chen, & Min, 2021). As shown in Fig. 1, the two air channels are separated by the middle sheets. The sheet transfers heat but prevents water content from infiltrating to the front channel (primary air channel). Water is delivered from the water reservoir and only sprayed to the rear channel (secondary air channel) from the top nozzles to generate water membrane on the channel surfaces. The moisture content difference between the flowing air and water film prompts water evaporation so as to remove the latent heat of the middle sheet, and the primary air in the adjacent

channel is then cooled.

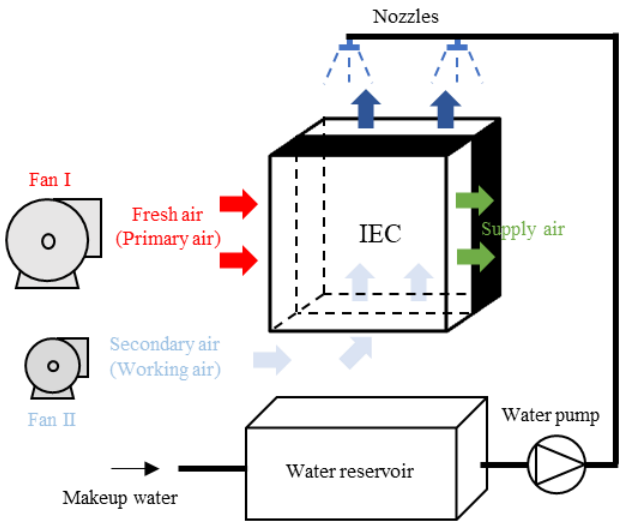

Fig. 1 Configuration of the cross-flow IEC with a pair of channels (Shi, Min, Ma, Chen, & Yang, 2022b)

Normally, the primary air is the outdoor fresh air, whereas the secondary air source of the IEC varies depending on the climatic conditions. In hot-dry regions, the outdoor air with relatively low relative humidity and wet-bulb temperature can be utilized as the secondary air (Q. Chen et al., 2021; Shi, Yang, Ma, & Liu, 2023). However, in hot and humid regions, the outdoor air with high humidity is not suitable for IEC secondary air. This limitation somewhat restricts the potential application of IEC systems in subtropical or tropical climatic conditions. Despite this constraint, the simple structure and high efficiency of this technology encourage researchers to explore alternative sources of secondary air so that IEC can contribute to energy saving in diverse climatic conditions. With the awareness of using the indoor exhaust air, the progress of the IEC unit and hybrid systems has been obtained through continuous efforts by researchers (Chakraborty, Vernon, Jha, & Narayanan, 2023; Zheng et al., 2019; Zhou, Yan, Dai, & Yu, 2022).

2. Literature review

Compared to traditional DEC which is applicable to certain hot-arid conditions (Xia, Han, Zhao, & Liang, 2021), the IEC has shown promising potential as a sustainable cooling approach in multiple zones, particularly in hot-humid regions (Shi, Ma, Gu, Min, & Yang, 2022). Published studies have shown that the IEC unit can get rid of the constraints of outdoor climate when using the indoor exhaust air with low temperature and humidity as the secondary air (Adam, Han, He, Amidpour, & Zhong, 2022; W. Li, Li, Shi, & Lu, 2021; Min, Chen, Shi, & Yang, 2021). In addition, the air in humid and hot areas has a higher dew point temperature than the wet-bulb temperature of indoor exhaust air, which means that condensation may occur in the primary air channels (Shahvari, Kalkhorani, & Clark, 2022; You, Wang, Guo, & Jiang, 2020). For instance, the model of the counter-flow IEC with dehumidification function has been proposed in hot-humid climate conditions, which can handle more cooling load compared with the sensible cooling operation mode (Y. Chen, Yang, & Luo, 2016). Three-dimensional IEC models were established considering the gradients of temperature and humidity in the channel gap, and the prediction accuracy was increased by 5.8% (Shi, Min, Chen, & Yang, 2022; Zhu, Chen, Zhang, & Wen, 2023). Comprehensive comparisons were carried out between the common types of IEC under both condensation and non-condensation states, revealing that the cooling performance of the counter-flow IEC was greater in theory (Min, Chen, & Yang, 2019). In order to diminish the additional thermal resistance due to the film condensation, Min et al. developed an IEC model with the hydrophobic coating on the surface of the primary air channel and verified it with experiments. The wet-bulb efficiency and dehumidification rate were 11.8% and 13.1% higher, respectively, than those of the normal IEC when using this functional material (Min, Shi, Shen, Chen, & Yang, 2021). Furthermore, spraying liquid desiccant (LD) onto the primary air channel was

investigated for the counter, cross, and counter-cross IECs for better water content removal. Cui et al. proposed an LD-based counter-flow IEC system and analyzed the effect of parameters on the outlet air status (Cui, Islam, Mohan, & Chua, 2016). Zhan et al. developed a simulation model of a cross-flow IEC with LD and validated it with experimental data. Results demonstrated that the heat transfer and dehumidification ratio of it are 1.3 and 2.9 times larger compared with the traditional IEC (H. Zhang, Ma, & Ma, 2021). Zhang et al. established a model of the LD-based IEC with hexagonal sheets, and performance was enhanced by 16% compared with the conventional one (Y. Zhang, Zhang, Yang, Chen, & Leung, 2022).

In addition to expanding the application range of the IEC unit, researchers have also been studying the hybrid systems that combine IEC with other devices to compensate for the insufficient cooling capacity of the IEC and guarantee the required supply air temperature. One example of an energy-saving approach in hot-humid climates is the use of an IEC as a pre-treatment unit for fresh air before it enters a vapor compression system (Cui, Chua, Islam, & Ng, 2015). Harrouz et al. developed a system that utilizes desiccant, dew point IEC, and the water reclamation unit. The system with metal-organic frameworks was shown to save more thermal and electrical energy, and the payback time was shorter as well (Harrouz, Katramiz, Ghali, Ouahrani, & Ghaddar, 2022). Duan et al. integrated the IEC with direct expansion (DX) and simulated it in a residential house. The energy consumption of the assembled system was 38.2% lower than that of the single DX (Duan, Zhao, Liu, & Zhang, 2019). Katramiz et al. combined the sustainable IEC unit with radiative cooling (RC) panel to process the air for a residential house under tropical desert climates. The system was demonstrated to consume less water resource than the single-stage IEC system and lower electricity than the typical AC system

(Katramiz et al., 2020). Nemati et al. combined an IEC with the underground air tunnel and evaluated it in theory under hot-arid weather conditions. Results revealed that the processed air of the system could handle the cooling load and maintain the indoor thermal environment, which replaced the traditional MVC system and saved 62% of energy (Nemati, Omidvar, & Rosti, 2021). Chen et al. proposed a hybrid system combining an IEC with a solar-assisted liquid desiccant dehumidifier. Solar heat is harvested for liquid regeneration, and the treated supply air can offset the latent load in the room area. The indoor AC system only needs to handle the sensible cooling load (Y. Chen, Yang, & Luo, 2018). Wan et al. hybridized an IEC with a latent heat storage system to treat the fresh air. The IEC was responsible for precooling, and the phase change material stored cooling from chilled water for further air cooling. The high efficiency and peak load shifting ability were both achieved by this system (Wan, Huang, Soh, & Jon Chua, 2023). Wang et al. proposed a ventilator using the IEC and a heat pump. The composite system was simulated in five representative cities of China, indicating that up to 85% of the cooling/heating load could be covered with less energy use (J. Wang, Lu, Li, Zeng, & Shi, 2022). The M-cycle evaporative cooler was combined with a solar-assisted solid desiccant system to handle the ambient air. Results showed that the proposed system achieved a 62.9% increase in energy savings and a 47% reduction in life cycle costs compared to traditional AC systems (Kousar, Ali, Sheikh, Gilani, & Khushnood, 2021). In general, although the IEC has been combined with a variety of equipment, it is currently mainly used in dry and hot areas, and the structure of the AC system in buildings is relatively simple.

Based on the current literature review, the following research gaps can be identified as the motivation of this study. Firstly, most hybrid IEC systems are studied under hot-arid climate regions,

whereas the hybrid IEC system is yet to be studied in hot-humid regions, although the recent development has overcome the climate barrier and expanded the IEC application. Secondly, the extant research mainly focused on the performance assessment of the hybrid IEC system as a single primary air handling unit (PAU) in residential buildings. In the case of commercial office buildings with high cooling loads, it is rare to solely rely on the fresh air system to meet the indoor cooling demand, as it is usually shared with the internal air conditioning system such as the fan coil unit (FCU) system. Nonetheless, existing studies have not established the entire building air conditioning system and analyzed the energy-saving effect when the IEC is adopted, especially in humid regions. In addition, the indoor thermal comfort and energy saving potentials need to be investigated when incorporating the IEC into the whole AC system, as well as to examine the associated economic and environmental issues.

The structure of this study is organized as follows. Firstly, the fresh air system integrated with the IEC that can be applied in hot-humid regions is described as an IEC-PAU. Secondly, the model of the hybrid AC system incorporating the IEC-PAU and FCUs is proposed constructed in an office building. A baseline system is also established for performance comparison. Thirdly, taking the cities of the Great Bay Area (GBA) as example cases, the energy saving potential of the IEC for the entire AC system is quantified considering different setpoint temperatures. The indoor thermal comfort is monitored to judge whether the proposed system could maintain a similar comfort level as the baseline system. Finally, the economic and environmental benefits of the IEC-PAU + FCU system are analyzed.

3. System description and model establishment

3.1 Description of the building AC system

Fig. 2 shows the schematic diagram of the building AC system on one floor. The IEC-PAU + indoor FCUs are proposed to work together for creating a comfortable indoor environment. The IEC-PAU is responsible for supplying the outdoor fresh air and handling the air to the status that has the same enthalpy as the indoor air-conditioned area. The outdoor free cooling can be employed to offset the internal heat gain in some days during the transition season. The indoor FCUs are fed with chilled water to cool the circulating room air, which mainly copes with the heat gain of building envelopes transferred from the external environment and the internal heat gain from occupants, lighting systems, and electrical equipment. A chiller produces chilled water for the IEC-PAU and FCUs, and the condenser side is connected to an external cooling tower for heat rejection. In addition, a baseline system that removes the IEC from the PAU is established with FCUs as well for comparison. In this reference case (PAU + FCU), the chilled water covers all the cooling load of the building.

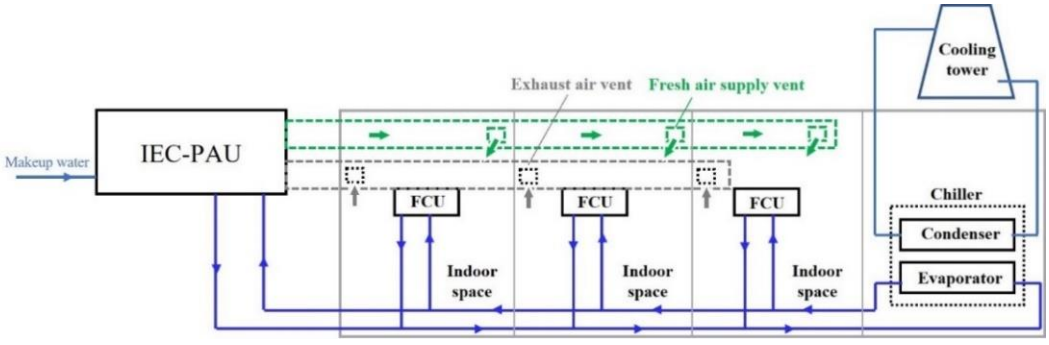

Fig. 2 Schematic diagram of the proposed hybrid IEC-PAU + FCUs system (The water splitter, mixer, and pumps are not presented)

The configuration of the IEC-PAU system is presented in Fig. 3, which comprises an IEC system and an auxiliary cooling coil section. When the system is operating, the fresh air is blown horizontally

from the left to the right side, passing through the IEC primary air channels and the coil section to be cooled in sequence. The secondary air flows along the grey dash duct. As mentioned in the Introduction part, the outdoor air in hot-humid regions is not suitable as the secondary air due to the massive moisture content, while the exhaust cool air from the indoor area can be the source of the secondary air in the IEC, which is not mixed with the fresh air. The water tank stores the circulated water that has flowed through the IEC channels without being evaporated and receives replenishment from the domestic water system. The chilled water will be delivered to the cooling coil to ensure a satisfactory supply air temperature. If the outdoor air is not high and humid, the cooling load from fresh air may be totally handled by the first-stage IEC unit. However, during the cooling season, when the cooling load is much heavier, the IEC and cooling coil are required to process the load together, which can result in condensation in both elements simultaneously.

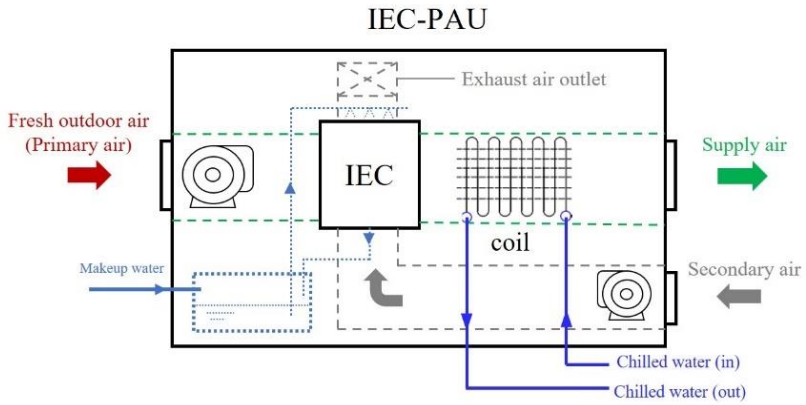

Fig. 3 The configuration of the IEC-PAU system

3.2 Model establishment framework

The framework for establishing the model is shown in Fig. 4. The main procedures can be outlined as follows. In the first place, the building physical model is built in Sketchup software, which provides the basic information such as the geometric dimensions and location of the opaque exterior elements

and fenestrations. Secondly, the physical model is endowed with thermal zones using the Openstudio plug-in module in Sketchup, which is subsequently input into Energyplus to assemble different modules in AC systems and to conduct year-round simulations in the building. The hourly weather data used in Energyplus is offered by the meteorological software of Meteonorm. The wet-bulb efficiency and dehumidification rate curves of the IEC are generated using a self-programmed code in Matlab software.

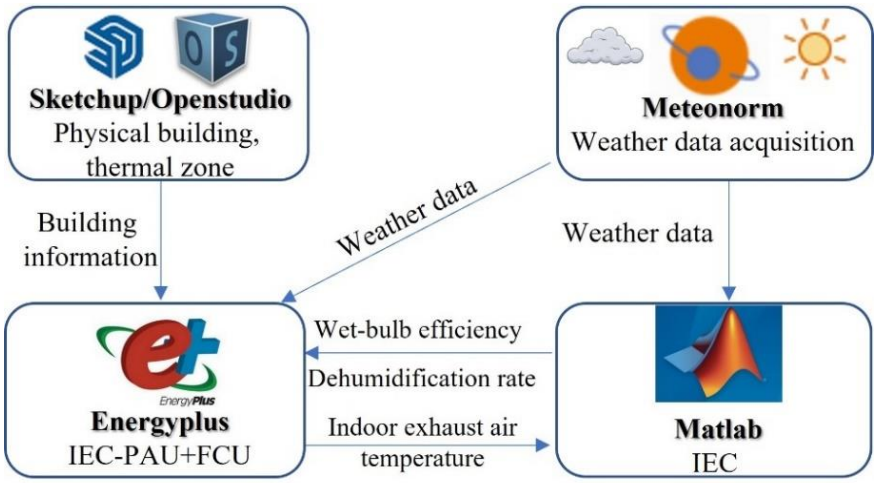

Fig. 4 The model establishment framework of this study

3.2.1 Physical model of the target building

As shown in Fig. 5, the physical model of the target building is from a reference building of the Department of Energy (DOE), which has been validated and used for energy analysis of the typical office building in China (H. Li et al., 2023; Zou et al., 2022). The essential geometric information and the thermal properties of the building envelopes are briefly listed in Table 1. The thermal properties of them have complied with the Chinese design standard of GB-50189 for energy conservation (MOHURD, 2015).

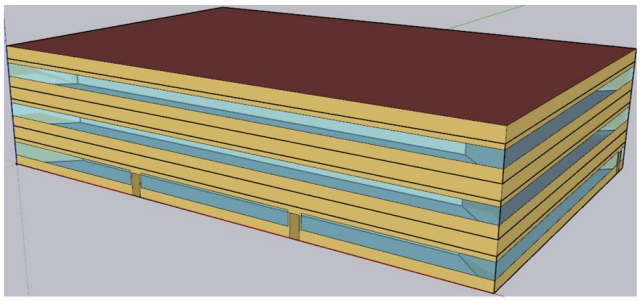

Fig. 5 Overview of the target office building

Table 1 Basic information of the building

Item	Value	Item	Value
Angle	0°	U-value of wall	0.435 W/(m^2·K)
Total floor area	4983 m^2	U-value of roof	0.282 W/(m^2·K)
Number of floors	3	U-value of door	2.101 W/(m^2·K)
Window-to-wall ratio	0.33	U-value of window	3.0 W/(m^2·K)
*L*W*H*	49.9 m*33.3 m*11.9 m	SHGC of window	0.29

3.2.2 System modeling and internal settings

In the target office building, an IEC-PAU is equipped on each floor to satisfy the fresh air requirement of the indoor personnel. The chilled water is supplied to the three IEC-PAUs and all FCUs from the ground to the top floors. The entire AC system model, consisting of the IEC-PAUs and the FCUs, is established using Energyplus. The air treatment of the IEC is simulated by the combination of the Evaporative Cooler: Indirect: Research Special module and the Heat exchanger: air-to-air: Sensible and Latent module. The former module operates when the IEC only handles the sensible load such as in some days of the transition seasons. The two modules are both active when the fresh air is hot and humid. In other words, the IEC handles sensible and latent cooling load simultaneously in this circumstance. The wet-bulb efficiency and dehumidification rate of the IEC follow the curves in Fig. 6. These curves are obtained by fitting the data from a validated cross-flow IEC model of our previous

study (Min et al., 2019), which can be expressed by Eq. (1) and Eq. (2). The indoor FCUs are modeled using the four-pipe fan coil module. The above modules are connected to form many small branches and loops according to their functions and nodes. These branches and loops are further organized to constitute the entire AC system in the target office building. The control policy of the proposed system is presented in Table 2. When the outdoor air is cool enough to offset the cooling load, water spraying of the IEC unit is not required, and the fresh air can be directly delivered into the indoor space. If the single-stage IEC with water spraying can able to handle the air to the status that has the same enthalpy as indoor air such as during the transition season, both IEC and FCUs should be turned on. In the summer time, the IEC-PAU and FCUs work together.

$$\eta_{wb}(m_{ratio}) = 0.05354m_{ratio}^3 - 0.2834m_{ratio}^2 + 0.6157m_{ratio} + 0.3831 \quad (1)$$

$$\varepsilon_{de}(m_{ratio}) = 0.002637m_{ratio}^3 - 0.04012m_{ratio}^2 + 0.1626m_{ratio} - 0.04283 \quad (2)$$

$$m_{ratio} = \frac{m_s}{m_p} \quad (3)$$

where η_{wb} is the wet-bulb efficiency of the IEC; ε_{de} is the dehumidification rate of the IEC; m_{ratio} is the mass ratio of secondary air to primary air.

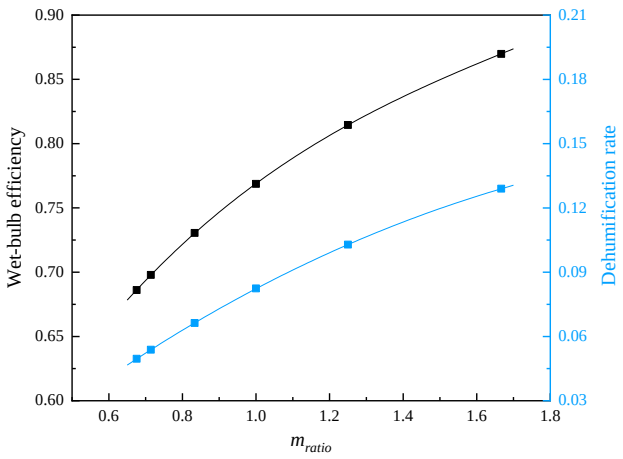

Fig. 6 Wet-bulb efficiency and dehumidification rate for the IEC

The general settings of people density, lighting, and electrical equipment are based on the national design code and technical handbook (CADG, 2022; MOHURD, 2012a). The values of each part are provided in Table 3. Two indicators, namely predicted mean vote (PMV) and predicted percentage of dissatisfied (PPD), are utilized for the evaluation of indoor thermal comfort when the proposed system and the baseline system are employed (Cheung, Schiavon, Parkinson, Li, & Brager, 2019). The recommended range of PMV can be determined from -1 (slightly cool) to 1 (slightly warm) (Duan et al., 2019).

Table 2 Control policy of the IEC-PAU + FCU system

Control mode	IEC		Coil (PAU)	FCU	Feature
	No water spray	Water spray			
I	●				Free cooling; Water spraying is not required; Outdoor air can be directly used to offset the cooling load.
II		●		●	IEC+FCU; Water spraying is required; IEC is able to handle the fresh air to the status that has the same enthalpy as indoor air; IEC and FCU work together.
III		●	●	●	IEC-PAU+FCU; The water spraying is required; IEC is not able to handle the fresh air to the status that has the same enthalpy as indoor air, which is combined with a coil as an IEC-PAU; IEC-PAU and FCU work together.

Table 3 General settings in the model

Item	Value
Occupant, m^2/person	7
Activity level	Extremely light
Fresh air volume, (m^3/h)/person	30

Thermal comfort	Fanger model (PMV, PPD)
Lighting, W/m^2	12
Electrical equipment, W/m^2	15
Operating schedule	8:00-19:00 (Mon.-Fri.) 8:00-14:00 (Sat.-Sun.)
Design indoor air temperature, ℃/relative humidity, %	24/60

Based on the general settings and the local weather conditions, the simulation results can be obtained for the two systems in the cities of GBA. For each case, the calculation procedures are summarized as follows. Firstly, the cooling load handled by the whole AC system is quantified, which can be divided into several components. Secondly, according to different setpoint temperatures, the comparisons of indoor thermal comfort and energy consumption between the IEC-PAU + FCU system and the baseline system are conducted, and the energy saving ratio can be calculated. Furthermore, the economic profits and environmental benefits are estimated for each scenario. In order to avoid repetition and make the content concise, the case of Shenzhen is taken as an example for detailed description, and the essential results of the other ten cities in GBA are presented and discussed after the illustrations of the Shenzhen case.

4. Results and discussion

4.1 Hourly weather conditions and cooling load

The hourly meteorological data of the city derives from Meteonorm software. Fig. 7 depicts the hourly variations of the outdoor air temperature (black curve) and relative humidity (green curve) throughout the year in Shenzhen (114.1° E, 22.55° N) when the AC system is in the operating period. The total working time is 3860 hours based on the operating schedule. It can be observed that the air

temperature generally increases in the middle of April and fluctuates around 29℃ from May, which starts to drop from the middle of October. The temperature remains above 15℃ in most of the time, while the minimum temperature is 6.9℃. Hence, Shenzhen has no central heating demand in winter, which is regarded as the single cooling domain. The relative humidity almost varies within the range of 65% and 100% from April to August, and it usually fluctuates between 40% and 100% in the other seven months.

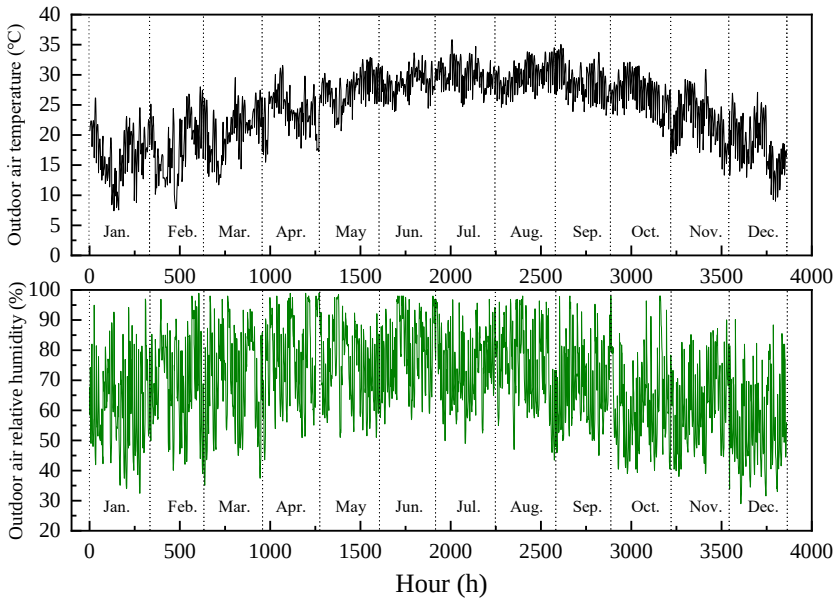

Fig. 7 The outdoor air temperature and relative humidity profile during the operating period in Shenzhen

Fig. 8 presents the hourly cumulative cooling load of the target building in the Shenzhen case. The greatest value of the cooling load is 480.1 kW. The total cooling load and fresh air load are the heaviest from June to August, which is also thick in early April, May to September, and early October. The fresh air load, which accounts for 36.8% of the total cooling load, is processed by IEC-PAU. The remaining load in the upper grey area is treated by the indoor FCU. The sensible load (orange area) and latent load (green area) handled by the IEC are 16.4% and 3.7% of the total cooling load,

respectively. Regarding the distribution of the handled cooling in the GBA cities, as seen from Fig. 9, the proportions of IEC sensible cooling (orange bar) vary in the range between 14.2% and 18.2% of the total load, which are higher in Guangzhou, Foshan, and Dongwan. The latent cooling of the IEC (green bar) accounts for 3.3% to 4.2% with greater values in Zhuhai, Macau, and Zhongshan. In addition, the PAU coil and indoor FCU are responsible for covering 14.0%-19.2% and 61.9%-66.7% of the total load, respectively, among the eleven cities.

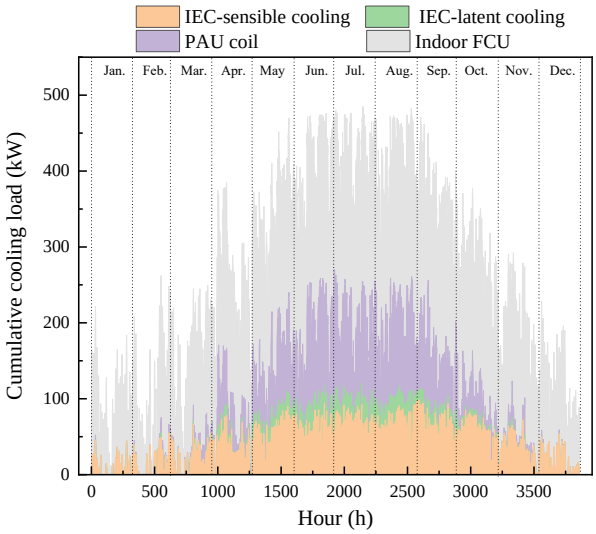

Fig. 8 The cooling load of the target building under weather conditions in Shenzhen

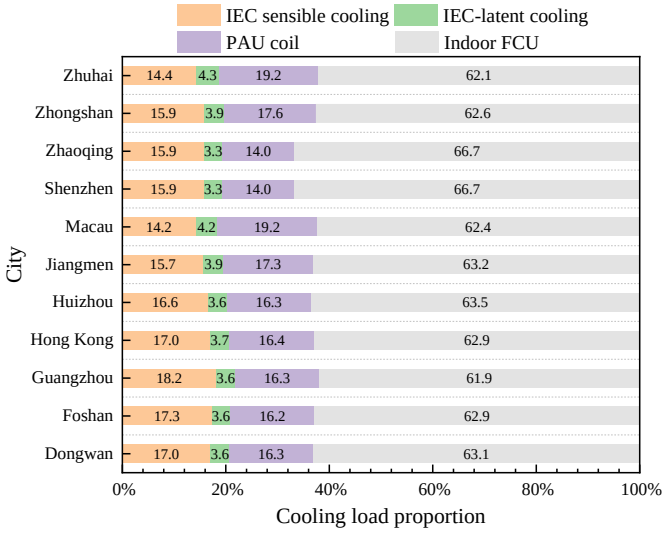

Fig. 9 Distributions of the handled cooling in different cities of GBA

4.2 Thermal comfort level and energy consumption

Before discussing the energy consumption of the AC systems, it is first necessary to evaluate the indoor personnel's thermal comfort level achieved by the proposed system as the ensured thermal comfort is the premise of energy consumption comparison. Therefore, the PMV and PPD are calculated for the IEC-PAU + FCU system and the reference system. The results of three rooms from the ground to the top floor are selected for the exhibition in figures. The PMV-PPD curves of the two systems are shown in Fig. 10. It can be noticed that the distributions of the points in the rooms on three floors are similar for both cases, indicating that the thermal environment can be stably maintained at a similar level by the proposed system as it is in the reference case. Furthermore, the cumulative hours with different ranges of PMV in Table 4 can demonstrate this issue as well. The values of cumulative hours within the PMV range from -1 to 1 are 3579 h, 3645 h, and 3618 h in the top-floor, middle-floor, and bottom-floor rooms, respectively, in the IEC-PAU + FCU case, which are close to them of 3599 h, 3662 h, and 3628 h in the reference case.

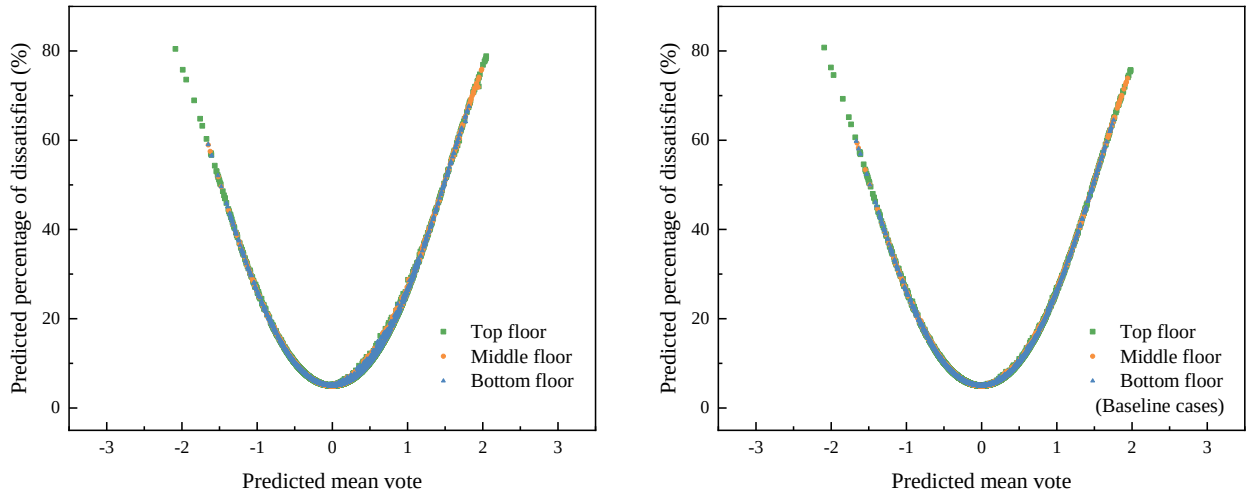

(a) (b)

Fig. 10 PMV and PPD of the selected rooms from the ground floor to the top floor (a) The IEC-PAU

+ FCU case (b) The baseline case

Table 4 The cumulative operating hour within different PMV scopes

Location		Top floor		Middle floor		Bottom floor	
System type		Baseline case	IEC-PAU + FCU	Baseline case	IEC-PAU + FCU	Baseline case	IEC-PAU + FCU
Cumulative hour of PMV ranges (h)	<-1	84	84	55	54	40	40
	[-1,1]	3599	3579	3662	3645	3628	3618
	>1	177	197	143	161	192	202
Satisfaction rate		97.80%	97.3%	99.5%	99.1%	98.6%	98.3%

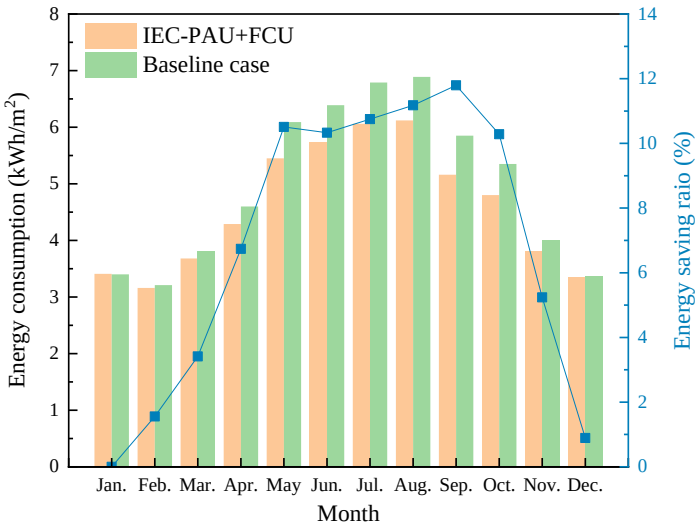

Fig. 11 The monthly energy consumption of the IEC-PAU + FCU system and the baseline system in the Shenzhen case

The monthly energy consumption of the IEC-PAU + FCU system and the reference system in the Shenzhen case throughout the year is compared in Fig. 11. It can be observed that the IEC-PAU + FCU system results in less energy demand than the baseline case in almost the whole year except in January. The greatest saving ratio is 11.8% in September, given the circumstance that the monthly energy consumption is reduced from 5.9 kWh/m^2 to 5.2 kWh/m^2 by the proposed system. Moreover, the

energy saving ratio is over 10% from May to October, indicating that the good performance can continue during the long and heavy cooling period. However, the differences of the consumed energy in January to March and December are relatively small, and less than 5% of energy can be saved. The reason is that the IEC-PAU only needs to undertake the role of providing fresh air in these months, while the function of air cooling is rarely active or even unnecessary, resulting in a relatively low energy saving ratio.

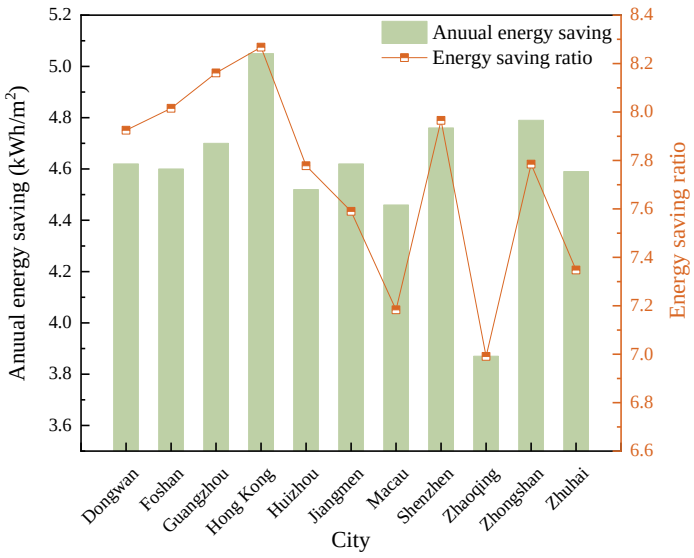

Fig. 12 The annual energy saving and energy saving ratio of the IEC-PAU+FCU system compared with the baseline system in different cities of GBA

Fig. 12 summarizes the annual energy saving and energy saving ratio achieved by the IEC-PAU + FCU system in the eleven GBA cities. The proposed system can reduce electrical energy consumption by an average of 4.6 kWh/m^2, and the higher values of annual energy saving are noticed in Hong Kong, Zhongshan, and Shenzhen, corresponding to 5.05 kWh/m^2, 4.79 kWh/m^2, and 4.76 kWh/m^2, respectively. It can be seen that Hong Kong has the maximum energy saving ratio of 8.3% among the eleven cities, followed by 8.2% in Guangzhou and 8.1% in Foshan. Nonetheless, the two

indicators of Zhaoqing both rank in the last place, which are 3.9 kWh/m^2 and 7.0% of energy saving and energy saving ratio, respectively.

4.3 Energy saving potential based on different setpoint temperatures

As discussed in section 4.2, it has been revealed that the IEC-PAU + FCU system can achieve the energy-saving benefits and maintain a stable indoor thermal environment. Nevertheless, the design indoor air setpoint may vary in a reasonable range with the local client requirements in practice. The change of the indoor air temperature can directly impact the status of the secondary air (exhaust air from indoor space), which in turn influences the wet-bulb efficiency and dehumidification rate of the IEC as well as the operation of other cooling devices in the entire AC system. Therefore, it is necessary to investigate the system performance under different indoor setpoints. Hence, the setpoint conditions of 25℃/60% and 26℃/60% are further input for calculation, which are commonly adopted in the system design (MOHURD, 2012b). If the secondary air conditions match either of the aforementioned two statuses, the corresponding wet-bulb efficiency and dehumidification rate curves of the IEC are written from Eq. (4) to Eq. (7), which are obtained in the same approach by fitting the results from the self-coded Matlab program, as mentioned in section 2.2.2.

$$\eta_{wb25℃}(m_{ratio}) = 0.06397m_{ratio}^3 - 0.3196\,{}^2_{ratio} + 0.6421m_{ratio} + 0.4054 \quad (4)$$

$$\varepsilon_{de25℃}(m_{ratio}) = -0.003569m_{ratio}^3 - 0.008858m_{ratio}^2 + 0.09956m_{ratio} - 0.03111 \quad (5)$$

$$\eta_{wb26℃}(m_{ratio}) = 0.08825m_{ratio}^3 - 0.41m_{ratio}^2 + 0.7351m_{ratio} + 0.4072 \quad (6)$$

$$\varepsilon_{de26℃}(m_{ratio}) = -0.01183m_{ratio}^3 + 0.03228m_{ratio}^2 + 0.1626m_{ratio} - 0.009595 \quad (7)$$

Similar to the previous scenario, the PMV and PPD values are monitored to ensure that the IEC-

PAU + FCU system maintains acceptable indoor thermal comfort levels, as in the reference case, under different temperature setpoints. The cumulative hours within the PMV range from -1 to 1 for the top-floor, middle-floor, and bottom-floor rooms are summarized in Table 5. It can be counted that the cumulative hours of the proposed system within the PMV range from -1 to 1 are almost the same in the top-floor room as in the baseline system when the setpoint temperatures are 25℃ and 26℃, and the satisfaction ratios in the middle and bottom floors are even slightly higher. Hence, the comparison of the energy consumption at the two setpoints can be carried out for the two AC systems.

Table 5 The cumulative operating hour within different PMV scopes

Location		Top floor			
System type		Baseline case		IEC-PAU + FCU	
Setpoint temperature (℃)		25	26	25	26
Cumulative hour of PMV ranges (h)	<-1	61	42	61	42
	[-1,1]	3306	3065	3298	3065
	>1	313	573	321	573
Satisfaction rate (%)		89.9%	83.3%	89.6%	83.3%
Location		Middle floor			
System type		Baseline case		IEC-PAU + FCU	
Setpoint temperature (℃)		25	26	25	26
Cumulative hour of PMV ranges (h)	<-1	18	9	19	9
	[-1,1]	3295	2985	3350	3082
	>1	367	686	311	589
Satisfaction rate (%)		89.5%	81.1%	91.0%	83.8%
Location		Bottom floor			
System type		Baseline case		IEC-PAU + FCU	

Setpoint temperature (℃)		25	26	25	26
Cumulative hour of PMV ranges (h)	<-1	34	22	35	22
	[-1,1]	3385	3095	3421	3224
	>1	261	563	224	434
Satisfaction rate (%)		92.0%	84.10%	93.0%	87.6%

After the confirmation of the acceptable thermal comfort level, the cooling load distributions and comparison of the energy consumptions are presented in Fig. 13 and Table 5. The IEC-PAU is responsible for treating 38.9% and 41.3% of the total cooling load, and the IEC can cover 18.6% and 18.1% of the total load given the indoor setpoints of 25℃ and 26℃, respectively. To handle the total cooling load, 51.9 kWh/m^2 and 48.9 kWh/m^2 of electrical energy are annually spent by the IEC-PAU + FCU system at the setpoints of 25℃ and 26℃, which are around 4.1 kWh/m^2 and 3.6 kWh/m^2 less than the reference case, respectively. As observed in Table 6, the saved energy and energy saving ratio both decrease with the increasing temperature, indicating that the saving potential of the proposed system is more suitable in the scenario with lower indoor setpoint values. Additionally, it is worth mentioning that the amount of reduced energy consumption by the proposed system is greater than the energy saved from raising 1℃ setpoint temperature in the baseline case. For instance, the amount of energy saving is 4.8 kWh/m^2 when the setpoint is 24℃ using the IEC-PAU + FCU system without sacrificing the thermal comfort, and it is better than 3.8 kWh/m^2 obtained by improving the temperature from 24℃ to 25℃ in the reference case. Similarly, the proposed system can reduce 4.1 kWh/m^2 of electricity consumption at the setpoint of 25℃, which is larger than 3.5 kWh/m^2 saved by raising the setpoint from 25℃ to 26℃ in the baseline system.

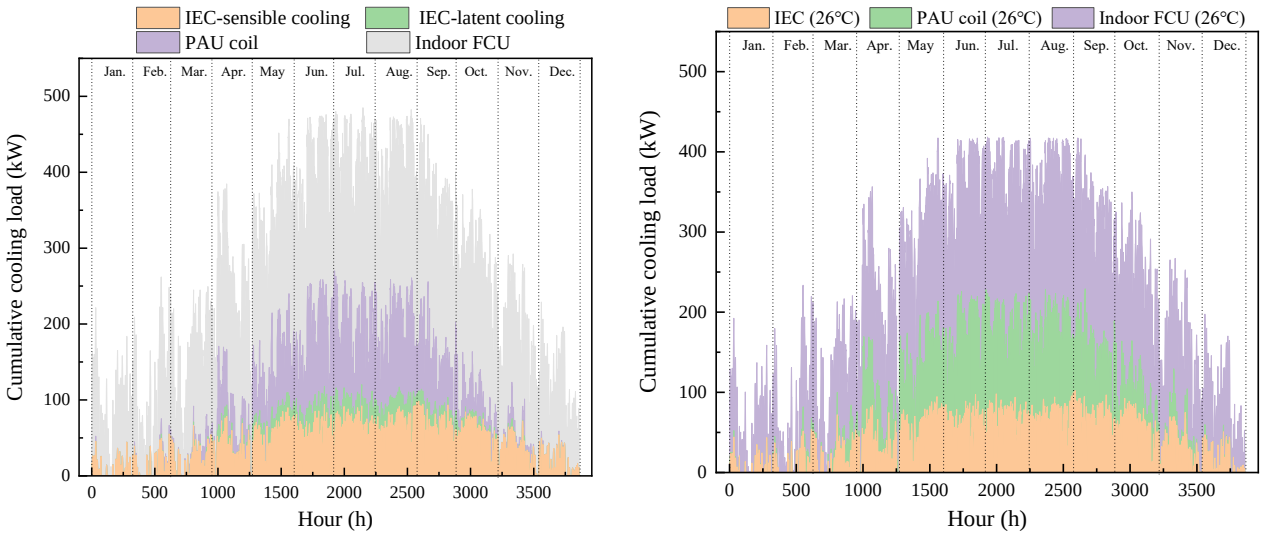

(a) Setpoint temperature: 25℃ (b) Setpoint temperature: 26℃

Fig. 13 Distribution of the handled load with different setpoint temperatures

Table 6 Comparison of the annual energy consumption between the IEC-PAU+FCU system and baseline system with different setpoint temperatures

Temperature setpoint (℃)	Energy consumption of the baseline case (kWh/m^2)	Energy consumption of IEC-PAU + FCU (kWh/m^2)	Energy saving (kWh/m^2)	Energy saving ratio
24	59.8	55	4.8	8.0%
25	56.0	51.9	4.1	7.3%
26	52.5	48.9	3.6	6.9%

Concerning the performance in the GBA cities, as shown in Fig. 14, the annual energy saving and energy saving ratio decrease with the higher setpoint value. When the setpoint is raised to 25℃, the saved energy drops from 4.6 kWh/m^2 to 4.0 kWh/m^2 on average, and it further lessens to 3.4 kWh/m^2 at 26℃. In respect to the individual performance, Hong Kong still has the highest values of the two indicators, which are 4.4 kWh/m^2 (7.7%) and 3.9 kWh/m^2 (7.2%) among the eleven cases given indoor temperatures of 25℃ and 26℃, respectively. Zhongshan and Shenzhen also show good performance

in energy saving. However, the results for Zhaoqing are in the last place again, with 3.4 kWh/m^2 (6.6%) and 2.5 kWh/m^2 (5.3%), which are far below the average levels.

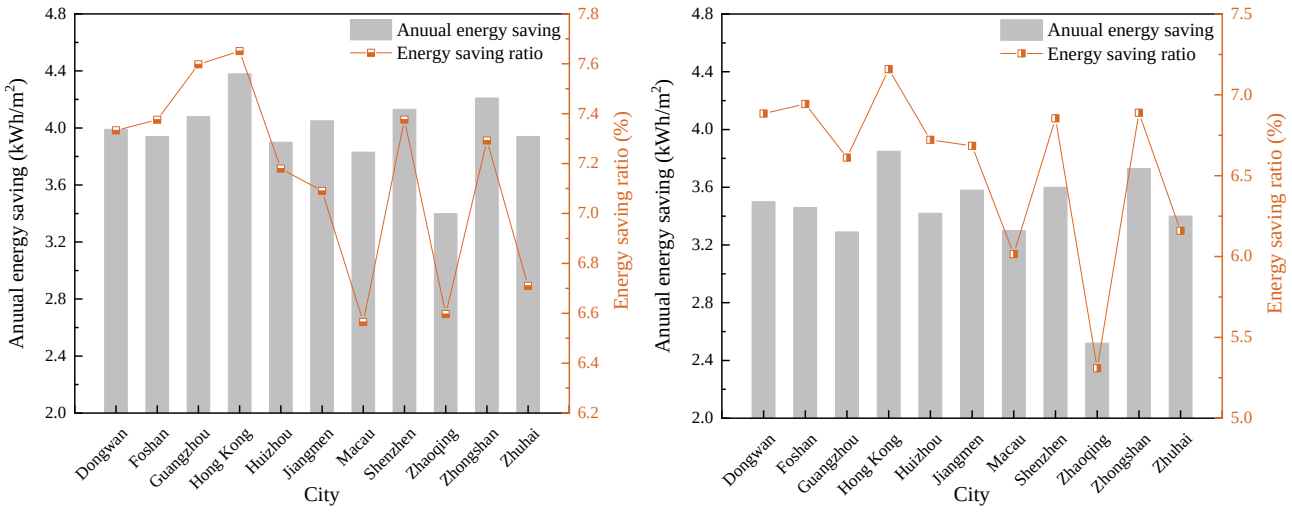

(a) Setpoint temperature: 25℃ (b) Setpoint temperature: 26℃

Fig. 14 Annual energy saving ratio of the IEC-PAU+FCU system at different setpoint temperatures in the GBA cities

4.4 Economic and environmental benefits

By and large, the above discussion can demonstrate that the IEC-PAU + FCU system can achieve energy saving at different setpoint temperatures compared with the reference case. Less energy consumption leads to lower energy charges and indirectly reduces the harmful emissions due to the usage of electricity. In this study, the net present value and discounted payback period are used to evaluate the economic benefit of the proposed system (H. Zhang, Ma, & Ma, 2022), and the environmental benefit is assessed by the greenhouse gas emission (Kousar, Ali, Amjad, & Ahmad, 2022).

The annual economic profit is evaluated by the net present value (NPV) (H. Zhang et al., 2022),

which is the value of the cash flows at the required rate of return by the proposed system compared with the reference case, as expressed by Eq. (8). By calculating the energy cost savings and subtracting the initial and maintenance costs, the cash inflow and outflow can be determined, respectively (Q. Wang, Pei, & Yang, 2021). In this study, the initial cost, which in fact is the additional cost due to the installation of an IEC system, is determined as 80000 CHY according to the market price.

$$NPV = -C_I + \sum_{j=1}^{n} \frac{C_{net}}{(1+r)^j} \tag{8}$$

where C_I is the initial cost of IEC, C_{net} is the net cash flow because of the saving of electricity charge by the proposed system, r is the discount rate, which is determined as 2.29%; j is the service life of the system, year.

The discounted payback period (DPP) takes into account the time value of money by discounting each cash flow before the cash flow is accumulated. It is the length of time that the cumulative discounted net cash savings of the IEC system can cover the initial cost of it until the NPV becomes positive, as formulated by Eq. (9). Energy saving varies with indoor setpoints and influences the profits. By examining recent electricity tariff trends in the GBA cities, a constant 5.5% annual increasing rate is determined. In addition, an annual regular maintenance cost of 1500 CHY for the IECs is involved. Considering the local tiered pricing for electricity listed in Appendix 1, the annual economic benefit and DPPs of the IEC-PAU + FCU system can be calculated for the eleven cities.

$$DPP = \frac{ln \frac{C_{net}}{C_{net} - rC_I}}{ln\,(1+r)} \tag{9}$$

Regarding the environmental benefit, the greenhouse gas (GHG) emission is a concerned issue

with the proposal of carbon peaking and carbon neutrality and can be obtained using Eq. (10). The GHG emission intensities in different cities are collected from the released document from the department of ecology and environment or sustainability reports from the local electricity company, which are 0.6379 kg CO_2 e/kWh, 0.57 kg CO_2 e/kWh, and 0.62 kg CO_2 e/kWh in GBA mainland cities, Hong Kong, and Macau, respectively (CEM, 2021; CLP, 2021; GPDEE, 2023).

$$M_{emission} = f_{emission} E \tag{10}$$

where $m_{emission}$ is the CO_2 emission ascribed to the usage of electricity, kg; $f_{emission}$ is the GHG emission intensity, kg CO_2 e/kWh; E is the annual energy saving of the proposed system, kWh.

Fig. 15 presents the economic and environmental benefits of the IEC-PAU + FCU system. The Hong Kong dollar (HKD) and Macau pataca (MOP) have been converted into CHY based on the current exchange rate to facilitate the comparison. As shown in Fig. 15(a), with a setpoint temperature of 24℃, one city (Hong Kong) can obtain more than 10000 CNY in profit, while six out of eleven cities can receive more than 9000 CNY in the first year by utilizing the IEC-PAU + FCU system. The average cash flow is 8953.3 CHY, and the maximum cash flow of 11549.8 CHY is observed in Hong Kong, which is attributed to the greatest amount of energy savings as well as the more expensive electricity tariff compared to mainland cities and Macau. The economic profits in Zhongshan and Guangzhou are also encouraging as 9569.6 CNY and 9402.7 CNY, ranking the second and the third place. In light of the greater cash flow, the DPPs in these cities are much shorter, which are 6.5 years (Hong Kong), 7.6 years (Zhongshan), and 7.8 years (Guangzhou). While the most extended DPP of 10.2 years is noticed in Zhaoqing due to the minimum economic profit of 6855.3 CHY, which is longer

than the average level of 8.2 years. In addition, an average greenhouse gas emission reduction of 4.8 t can be achieved annually in the GBA cities. Zhongshan (5.1 t), Shenzhen (5.0 t), and Guangzhou (5.0 t) perform better and rank in the top three.

When the setpoint temperature is increased to 25℃ and 26℃, it can be realized from Fig. 15(b)-(c) that the economic benefits noticeably shrink because less energy is saved by the proposed system, and the DPPs are inevitably prolonged. The average cash flows are reduced to 7697.2 CNY and 6689.2 CNY, accompanied with the expanded average DPPs of 9.4 years and 10.6 years, respectively, across the GBA cities. With regards to the performance of individuals, the income of the Hong Kong case decreases from 9958.4 CNY to 8684.3 CNY, and the DPP increases from 7.4 years to 8.3 years, accompanied by the reduced CO_2 emission reductions from 4.2 t to 3.7 t. Only three cities have the net cash flows beyond 8000 CNY at the setpoint of 25℃, and three cities can achieve over the annual profit of 7000 CHY if the setpoint is 26℃. The longer DPPs are a result of lower profits, which are extended to more than ten years in eight cities.

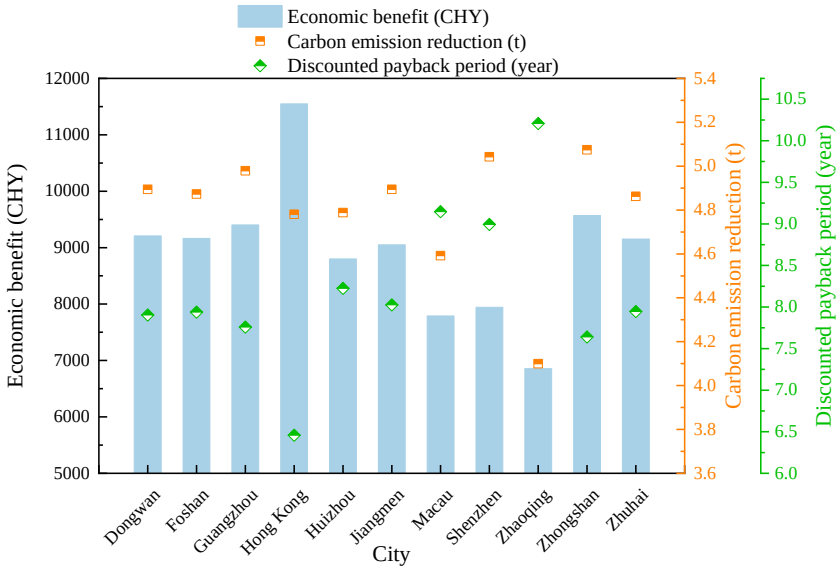

(a) Setpoint temperature: 24℃

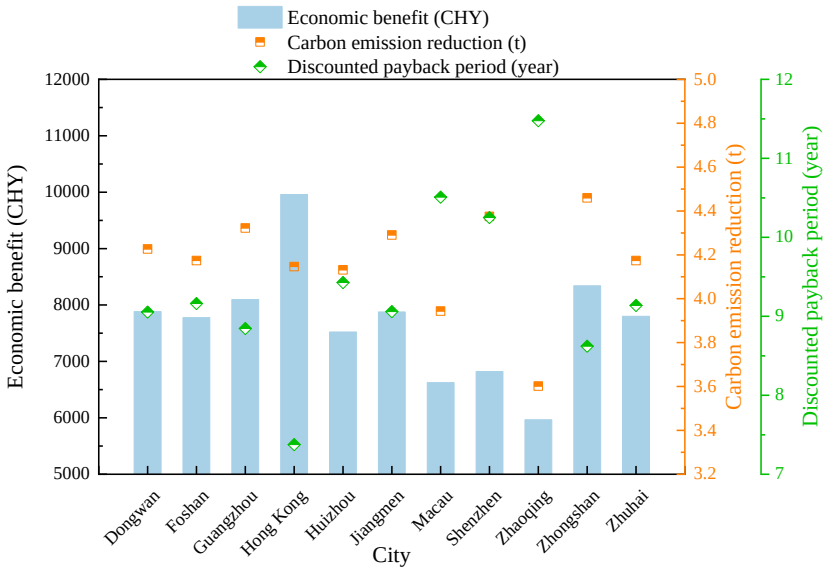

(b) Setpoint temperature: 25℃

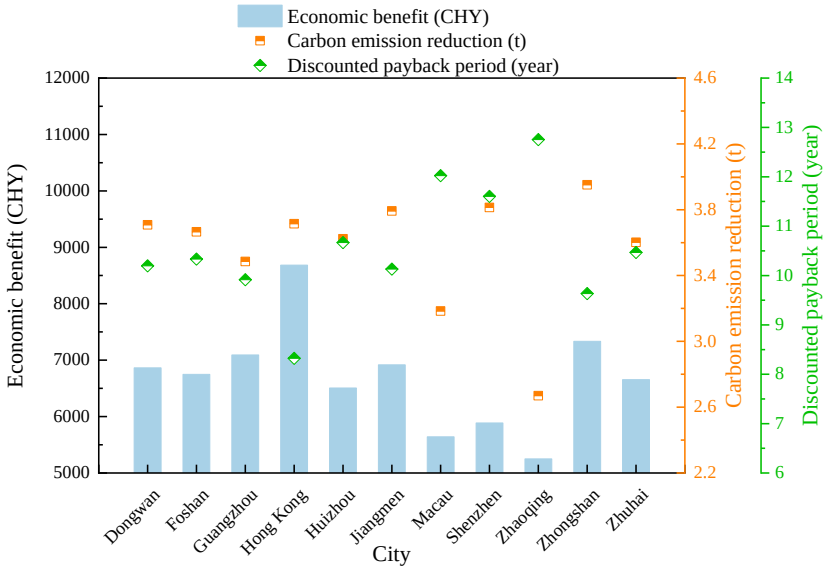

(c) Setpoint temperature: 26℃

Fig. 15 The economic and environmental benefits of IEC-PAU + FCU compared with the baseline case in the GBA cities

5. Conclusions

In this study, a hybrid indirect evaporative cooling (IEC) system with indoor fan coil units (FCUs) is proposed for a typical office building in hot-humid areas. The IEC is integrated with a cooling coil

as the primary air handling unit (IEC-PAU), which works together with FCUs for maintaining the indoor thermal environment. Before evaluating the energy-saving effect of the IEC-PAU + FCU system, the thermal comfort is monitored to ensure it remains within the acceptable level as it is of the reference case. The performance of the two air conditioning systems is then compared based on weather conditions of the Great Bay Area (GBA) cities in China considering different temperature setpoints. Eventually, the economic and environmental benefits of the proposed system are presented. The main findings are summarized as follows.

1) The monthly energy consumption of the IEC-PAU + FCU system is lower for almost the whole year compared with the reference system. The effective month can continue for a half year from May to October with monthly energy saving ratios over 10%, which coincides the heavy cooling load periods in the year.

2) The IEC-PAU + FCU system can reduce energy consumption within the acceptable thermal comfort range as it is in the baseline case. The greatest energy saving ratio is 8.3% among the GBA cities. However, its energy saving performance decreases as the setpoint temperature increases. The dwindled electricity usage is 4.6 kWh/m^2 on average when the setpoint temperature is 24℃, which drops rapidly to 4.0 kWh/m^2 and 3.4 kWh/m^2, respectively, at the setpoints of 25℃ and 26℃.

3) The economic benefit of the IEC-PAU + FCU system is dependent on energy savings and local electricity tariffs. The greatest annual net cash flow of 11549.8 CHY is achieved in Hong Kong, owing to the maximum energy saving as well as the more expensive electricity tariff than mainland cities and Macau. The economic benefits in Zhongshan and Guangzhou rank second and third,

which are both beyond the average level of 8953.3 CHY. The average discounted payback period (DPP) is 8.2 years, while it is extended to more than ten years with the increasing setpoint temperature of 26℃.

4) For the environmental benefit, an average CO_2 emission of 4.8 t can be annually reduced in the GBA cities. Zhongshan (5.1 t), Shenzhen (5.0 t), and Guangzhou (5.0 t) perform better by the IEC-PAU + FCU system compared with the reference case.

In summary, this work demonstrates the feasibility of the hybrid IEC system as an effective approach for energy saving in hot-humid regions, which is also conducive to achieving the carbon neutrality in China.

Appendix A1 The electricity tariff in the GBA cities

Table A1-1 Daily electricity tariff in GBA cities (CEM, 2022; CLP, 2023; CSPGC, 2023)

City	Peak [1]	Peak [2]	Normal period	Valley [3]
Dongwan	172.026875	138.176875	82.416875	33.036875
Foshan	172.026875	138.176875	82.416875	33.036875
Guangzhou	172.026875	138.176875	82.416875	33.036875
Hong Kong	143.637 [4]			
Huizhou	168.416875	135.286875	80.716875	32.386875
Jiangmen	169.056875	135.796875	81.016875	32.506875
Macau	116.358 [5]			
Shenzhen	139.396875	111.2669	82.82688	25.73688
Zhaoqing	154.546875	124.186875	74.186875	29.906875
Zhongshan	172.026875	138.176875	82.416875	33.036875
Zhuhai	172.026875	138.176875	82.416875	33.036875

Note:

(1) Only 11:00-12:00 and 15:00-17:00 from July to September

(2) 10:00-12:00, 14:00-19:00 every day

(3) 0:00-8:00 every day

(4) Converted from HKD into CHY.

(5) Converted from MOP into CHY.

Based on the yearly variation of the electricity tariff in these GBA cities, the annual increasing rate of 5.5% is also considered when the DPP is calculated.

CRediT authorship contribution statement

Wenchao Shi: Conceptualization; Methodology; Program; Formal analysis; Writing – original draft. **Hongxing Yang:** Conceptualization; Supervision; Funding acquisition; Writing – review & editing; **Xiaochen Ma:** Validation; Data curation; Resources; **Xiaohua Liu:** Writing – review & editing; Supervision.

Declaration of competing interest

The authors declare that they have no known competing financial interests or personal relationships that could have appeared to influence the work reported in this paper.

Acknowledgment

The authors wish to acknowledge the financial support provided by the General Research Fund projects of the Hong Kong Research Grant Council (Ref. No.: 15213219 and 15200420).

References

Abaranji, S., Panchabikesan, K., & Ramalingam, V. (2021). Experimental study on the direct evaporative air-cooling system with vermicompost material as the water storage medium. *Sustainable Cities and Society, 71*, 102991. Retrieved from https://www.sciencedirect.com/science/article/pii/S2210670721002778. doi:https://doi.org/10.1016/j.scs.2021.102991

Adam, A., Han, D., He, W., Amidpour, M., & Zhong, H. (2022). Numerical investigation of the heat and mass transfer process within a cross-flow indirect evaporative cooling system for hot and humid climates. *Journal of Building Engineering, 45*, 103499. Retrieved from https://www.sciencedirect.com/science/article/pii/S2352710221013577. doi:https://doi.org/10.1016/j.jobe.2021.103499

CADG. (2022). Technical measurement of heating ventilation and air conditioning design for civil buildings 2022.

CEM. (2021). Sustainability development report. Retrieved from https://www.cem-macau.com/uploads/pdf_sustainability_report_2021_zh_686f6a3e9a.pdf

CEM. (2022). Tariff Group A. *Companhia de Electricidade de Macau.* Retrieved from https://www.cem-macau.com/zh/customer-service/billing-service/tariff-group-a/

Chakraborty, S., Vernon, D., Jha, A., & Narayanan, V. (2023). Performance characterization of M-cycle indirect evaporative cooler and heat recovery ventilator for commercial buildings – Experiments and model. *Energy and Buildings, 281*, 112762. Retrieved from https://www.sciencedirect.com/science/article/pii/S0378778822009331. doi:https://doi.org/10.1016/j.enbuild.2022.112762

Chen, Q., Kum Ja, M., Burhan, M., Akhtar, F. H., Shahzad, M. W., Ybyraiymkul, D., & Ng, K. C. (2021). A hybrid indirect evaporative cooling-mechanical vapor compression process for energy-efficient air conditioning. *Energy Conversion and Management, 248*, 114798. Retrieved from https://www.sciencedirect.com/science/article/pii/S0196890421009742. doi:https://doi.org/10.1016/j.enconman.2021.114798

Chen, Y., Yang, H., & Luo, Y. (2016). Indirect evaporative cooler considering condensation from primary air: Model development and parameter analysis. *Building and Environment, 95*, 330-345. Retrieved from https://www.sciencedirect.com/science/article/pii/S0360132315301396. doi:https://doi.org/10.1016/j.buildenv.2015.09.030

Chen, Y., Yang, H., & Luo, Y. (2018). Investigation on solar assisted liquid desiccant dehumidifier and evaporative cooling system for fresh air treatment. *Energy, 143*, 114-127. Retrieved from https://www.sciencedirect.com/science/article/pii/S0360544217318297. doi:https://doi.org/10.1016/j.energy.2017.10.124

Cheung, T., Schiavon, S., Parkinson, T., Li, P., & Brager, G. (2019). Analysis of the accuracy on PMV – PPD model using the ASHRAE Global Thermal Comfort Database II. *Building and Environment, 153*, 205-217. Retrieved from https://www.sciencedirect.com/science/article/pii/S0360132319300915. doi:https://doi.org/10.1016/j.buildenv.2019.01.055

CLP. (2021). Sustainability report 120 years of shared version. *CHINA ELECTRIC EQUIPMENT GROUP (HONG KONG) LIMITED.* Retrieved from

https://www.clpgroup.com/content/dam/clp-group/channels/sustainability/document/sustainability-report/2021/CLP_Sustainability_Report_2021_en.pdf.coredownload.pdf

CLP. (2023). 2023 Tariff Adjustment Retrieved from https://www.clp.com.hk/en/clp-power-tariff-adjustment-20221

CSPGC. (2023). Announcement of Guangdong Power Grid Co., Ltd. on the price of commercial users purchasing electricians as agents in February 2023. http://www.conghua.gov.cn/gzchkgsx/attachment/7/7229/7229252/8789235.pdf

Cui, X., Chua, K. J., Islam, M. R., & Ng, K. C. (2015). Performance evaluation of an indirect pre-cooling evaporative heat exchanger operating in hot and humid climate. *Energy Conversion and Management, 102*, 140-150. Retrieved from https://www.sciencedirect.com/science/article/pii/S0196890415001387. doi:https://doi.org/10.1016/j.enconman.2015.02.025

Cui, X., Islam, M. R., Mohan, B., & Chua, K. J. (2016). Theoretical analysis of a liquid desiccant based indirect evaporative cooling system. *Energy, 95*, 303-312. Retrieved from https://www.sciencedirect.com/science/article/pii/S0360544215016746. doi:https://doi.org/10.1016/j.energy.2015.12.032

Duan, Z., Zhao, X., Liu, J., & Zhang, Q. (2019). Dynamic simulation of a hybrid dew point evaporative cooler and vapour compression refrigerated system for a building using EnergyPlus. *Journal of Building Engineering, 21*, 287-301. Retrieved from https://www.sciencedirect.com/science/article/pii/S2352710218305230. doi:https://doi.org/10.1016/j.jobe.2018.10.028

GPDEE. (2023). *Notice on the Verification and Quota Clearance of Carbon Emissions Reports for Provincial Controlled Enterprises in 2022*. Guangdong Province, China Retrieved from http://gdee.gd.gov.cn/attachment/0/515/515612/4148564.pdf

Harrouz, J. P., Katramiz, E., Ghali, K., Ouahrani, D., & Ghaddar, N. (2022). Life cycle assessment of desiccant – Dew point evaporative cooling systems with water reclamation for poultry houses in hot and humid climate. *Applied Thermal Engineering, 210*, 118419. Retrieved from https://www.sciencedirect.com/science/article/pii/S135943112200374X. doi:https://doi.org/10.1016/j.applthermaleng.2022.118419

Katramiz, E., Al Jebaei, H., Alotaibi, S., Chakroun, W., Ghaddar, N., & Ghali, K. (2020). Sustainable cooling system for Kuwait hot climate combining diurnal radiative cooling and indirect evaporative cooling system. *Energy, 213*, 119045. Retrieved from https://www.sciencedirect.com/science/article/pii/S0360544220321526. doi:https://doi.org/10.1016/j.energy.2020.119045

Kousar, R., Ali, M., Amjad, M. K., & Ahmad, W. (2022). Energy, Exergy, Economic, Environmental (4Es) comparative performance evaluation of dewpoint evaporative cooler configurations. *Journal of Building Engineering, 45*, 103466. Retrieved from https://www.sciencedirect.com/science/article/pii/S2352710221013243. doi:https://doi.org/10.1016/j.jobe.2021.103466

Kousar, R., Ali, M., Sheikh, N. A., Gilani, S. I. u. H., & Khushnood, S. (2021). Holistic integration of multi-stage dew point counter flow indirect evaporative cooler with the solar-assisted desiccant

cooling system: A techno-economic evaluation. *Energy for Sustainable Development, 62*, 163-174. Retrieved from https://www.sciencedirect.com/science/article/pii/S097308262100051X. doi:https://doi.org/10.1016/j.esd.2021.04.005

Li, H., Li, J., Li, S., Peng, J., Ji, J., & Yan, J. (2023). Matching characteristics and AC performance of the photovoltaic-driven air conditioning system. *Energy, 264*. doi:10.1016/j.energy.2022.126509

Li, W., Li, Y., Shi, W., & Lu, J. (2021). Energy and exergy study on indirect evaporative cooler used in exhaust air heat recovery. *Energy, 235*, 121319. Retrieved from https://www.sciencedirect.com/science/article/pii/S036054422101567X. doi:https://doi.org/10.1016/j.energy.2021.121319

Liu, X., Liu, X., Jiang, Y., Zhang, T., & Hao, B. (2022). PEDF (photovoltaics, energy storage, direct current, flexibility), a power distribution system of buildings for grid decarbonization: Definition, technology review, and application. *CSEE Journal of Power and Energy Systems*, 1-18. doi:10.17775/CSEEJPES.2022.04850

Men, Y., Liu, X., & Zhang, T. (2021). A review of boiler waste heat recovery technologies in the medium-low temperature range. *Energy, 237*, 121560. Retrieved from https://www.sciencedirect.com/science/article/pii/S0360544221018089. doi:https://doi.org/10.1016/j.energy.2021.121560

Min, Y., Chen, Y., Shi, W., & Yang, H. (2021). Applicability of indirect evaporative cooler for energy recovery in hot and humid areas: Comparison with heat recovery wheel. *Applied Energy, 287*. doi:10.1016/j.apenergy.2021.116607

Min, Y., Chen, Y., & Yang, H. (2019). Numerical study on indirect evaporative coolers considering condensation: A thorough comparison between cross flow and counter flow. *International Journal of Heat and Mass Transfer, 131*, 472-486. Retrieved from https://www.sciencedirect.com/science/article/pii/S001793101834002X. doi:https://doi.org/10.1016/j.ijheatmasstransfer.2018.11.082

Min, Y., Shi, W., Shen, B., Chen, Y., & Yang, H. (2021). Enhancing the cooling and dehumidification performance of indirect evaporative cooler by hydrophobic-coated primary air channels. *International Journal of Heat and Mass Transfer, 179*, 121733. Retrieved from https://www.sciencedirect.com/science/article/pii/S0017931021008395. doi:https://doi.org/10.1016/j.ijheatmasstransfer.2021.121733

Mirzazade Akbarpoor, A., Moghtader Gilvaei, Z., Haghighi Poshtiri, A., & Zhong, L. (2022). A hybrid domed roof and evaporative cooling system: thermal comfort and building energy evaluation. *Sustainable Cities and Society, 80*, 103756. Retrieved from https://www.sciencedirect.com/science/article/pii/S2210670722000877. doi:https://doi.org/10.1016/j.scs.2022.103756

MOHURD. (2012a). Design code for heating ventilation and air conditioning of civil buildings. *GB50736-2012*.

MOHURD. (2012b). Design code for heating ventilation and air conditioning of civil buildings (GB50736). *Beijing, China*.

MOHURD. (2015). Design standard for energy efficiency of public buildings. *GB50189-2015*.

Nemati, N., Omidvar, A., & Rosti, B. (2021). Performance evaluation of a novel hybrid cooling system

combining indirect evaporative cooler and earth-air heat exchanger. *Energy, 215*, 119216. Retrieved from https://www.sciencedirect.com/science/article/pii/S0360544220323239. doi:https://doi.org/10.1016/j.energy.2020.119216

Shahvari, S. Z., Kalkhorani, V. A., & Clark, J. D. (2022). Performance evaluation of a metal organic frameworks based combined dehumidification and indirect evaporative cooling system in different climates. *International Journal of Refrigeration, 140*, 186-197. Retrieved from https://www.sciencedirect.com/science/article/pii/S0140700722001530. doi:https://doi.org/10.1016/j.ijrefrig.2022.05.001

Shi, W., Ma, X., Gu, Y., Min, Y., & Yang, H. (2022). Indirect evaporative cooling maps of China: Optimal and quick performance identification based on a data-driven model. *Energy Conversion and Management, 268*, 116047. Retrieved from https://www.sciencedirect.com/science/article/pii/S0196890422008366. doi:https://doi.org/10.1016/j.enconman.2022.116047

Shi, W., Min, Y., Chen, Y., & Yang, H. (2022). Development of a three-dimensional numerical model of indirect evaporative cooler incorporating with air dehumidification. *International Journal of Heat and Mass Transfer, 185*, 122316. Retrieved from https://www.sciencedirect.com/science/article/pii/S0017931021014150. doi:https://doi.org/10.1016/j.ijheatmasstransfer.2021.122316

Shi, W., Min, Y., Ma, X., Chen, Y., & Yang, H. (2022a). Dynamic performance evaluation of porous indirect evaporative cooling system with intermittent spraying strategies. *Applied Energy, 311*. doi:10.1016/j.apenergy.2022.118598

Shi, W., Min, Y., Ma, X., Chen, Y., & Yang, H. (2022b). Performance evaluation of a novel plate-type porous indirect evaporative cooling system: An experimental study. *Journal of Building Engineering, 48*, 103898. Retrieved from https://www.sciencedirect.com/science/article/pii/S2352710221017563. doi:https://doi.org/10.1016/j.jobe.2021.103898

Shi, W., Yang, H., Ma, X., & Liu, X. (2023). A novel indirect evaporative cooler with porous media under dual spraying modes: A comparative analysis from energy, exergy, and environmental perspectives. *Journal of Building Engineering*, 106874. Retrieved from https://www.sciencedirect.com/science/article/pii/S2352710223010537. doi:https://doi.org/10.1016/j.jobe.2023.106874

Sun, T., Tang, T., Yang, C., Yan, W., Cui, X., & Chu, J. (2023). Cooling performance and optimization of a tubular indirect evaporative cooler based on response surface methodology. *Energy and Buildings*, 112880. Retrieved from https://www.sciencedirect.com/science/article/pii/S037877882300110X. doi:https://doi.org/10.1016/j.enbuild.2023.112880

Tariq, R., Sheikh, N. A., Livas-García, A., Xamán, J., Bassam, A., & Maisotsenko, V. (2021). Projecting global water footprints diminution of a dew-point cooling system: Sustainability approach assisted with energetic and economic assessment. *Renewable and Sustainable Energy Reviews, 140*, 110741. Retrieved from https://www.sciencedirect.com/science/article/pii/S136403212100037X. doi:https://doi.org/10.1016/j.rser.2021.110741

Wan, Y., Huang, Z., Soh, A., & Jon Chua, K. (2023). On the performance study of a hybrid indirect evaporative cooling and latent-heat thermal energy storage system under commercial operating conditions. *Applied Thermal Engineering, 221*, 119902. Retrieved from https://www.sciencedirect.com/science/article/pii/S1359431122018324. doi:https://doi.org/10.1016/j.applthermaleng.2022.119902

Wang, J., Lu, J., Li, W., Zeng, C., & Shi, F. (2022). Numerical study on performance of a hybrid indirect evaporative cooling heat recovery heat pump ventilator as applied in different climatic regions of China. *Energy, 239*, 122431. Retrieved from https://www.sciencedirect.com/science/article/pii/S0360544221026803. doi:https://doi.org/10.1016/j.energy.2021.122431

Wang, Q., Pei, G., & Yang, H. (2021). Techno-economic assessment of performance-enhanced parabolic trough receiver in concentrated solar power plants. *Renewable Energy, 167*, 629-643. Retrieved from https://www.sciencedirect.com/science/article/pii/S096014812031884X. doi:https://doi.org/10.1016/j.renene.2020.11.132

Xia, B., Han, J., Zhao, J., & Liang, K. (2021). Technological adaptation zone of passive evaporative cooling of China, based on a clustering analysis. *Sustainable Cities and Society, 66*, 102564. Retrieved from https://www.sciencedirect.com/science/article/pii/S2210670720307824. doi:https://doi.org/10.1016/j.scs.2020.102564

Yang, H., Shi, W., Chen, Y., & Min, Y. (2021). Research development of indirect evaporative cooling technology: An updated review. *Renewable and Sustainable Energy Reviews, 145*, 111082. Retrieved from https://www.sciencedirect.com/science/article/pii/S1364032121003701. doi:https://doi.org/10.1016/j.rser.2021.111082

You, Y., Wang, G., Guo, C., & Jiang, H. (2020). Study on mass transfer time relaxation parameter of indirect evaporative cooler considering primary air condensation. *Applied Thermal Engineering, 181*, 115958. Retrieved from https://www.sciencedirect.com/science/article/pii/S1359431120334402. doi:https://doi.org/10.1016/j.applthermaleng.2020.115958

Zhang, H., Ma, H., & Ma, S. (2021). Investigation on indirect evaporative cooling system integrated with liquid dehumidification. *Energy and Buildings, 249*, 111179. Retrieved from https://www.sciencedirect.com/science/article/pii/S0378778821004631. doi:https://doi.org/10.1016/j.enbuild.2021.111179

Zhang, H., Ma, H., & Ma, S. (2022). Energy, exergy, economic and environmental analysis of an indirect evaporative cooling integrated with liquid dehumidification. *Energy, 253*, 124147. Retrieved from https://www.sciencedirect.com/science/article/pii/S0360544222010507. doi:https://doi.org/10.1016/j.energy.2022.124147

Zhang, Y., Zhang, H., Yang, H., Chen, Y., & Leung, C. W. (2022). Counter-crossflow indirect evaporative cooling-assisted liquid desiccant dehumidifier: Model development and parameter analysis. *Applied Thermal Engineering, 217*, 119231. Retrieved from https://www.sciencedirect.com/science/article/pii/S1359431122011619. doi:https://doi.org/10.1016/j.applthermaleng.2022.119231

Zheng, B., Guo, C., Chen, T., Shi, Q., Lv, J., & You, Y. (2019). Development of an experimental validated model of cross-flow indirect evaporative cooler with condensation. *Applied Energy,*

252, 113438. Retrieved from https://www.sciencedirect.com/science/article/pii/S0306261919311122. doi:https://doi.org/10.1016/j.apenergy.2019.113438

Zhou, Y., Yan, Z., Dai, Q., & Yu, Y. (2022). Experimental study on the performance of a novel hybrid indirect evaporative cooling/thermoelectric cooling system. *Building and Environment, 207*, 108539. Retrieved from https://www.sciencedirect.com/science/article/pii/S036013232100932X. doi:https://doi.org/10.1016/j.buildenv.2021.108539

Zhu, G., Chen, W., Zhang, D., & Wen, T. (2023). Performance evaluation of counter flow dew-point evaporative cooler with a three-dimensional numerical model. *Applied Thermal Engineering, 219*, 119483. Retrieved from https://www.sciencedirect.com/science/article/pii/S1359431122014132. doi:https://doi.org/10.1016/j.applthermaleng.2022.119483

Zou, B., Peng, J., Yin, R., Li, H., Li, S., Yan, J., & Yang, H. (2022). Capacity configuration of distributed photovoltaic and battery system for office buildings considering uncertainties. *Applied Energy, 319*. doi:10.1016/j.apenergy.2022.119243